Biosensors and Bioelectronics 49 (2013) 341–347

Contents lists available at SciVerse ScienceDirect

Biosensors and Bioelectronics

journal homepage: www.elsevier.com/locate/bios

Short communication

Fast nonlinear region localisation for nonlinear dielectric spectroscopy of biological suspensions

Gabriel A. Ruiz [a,*], Carmelo J. Felice [a,b]

[a] Laboratorio de Medios e Interfases, Departamento de Bioingeniería, Facultad de Ciencias Exactas y Tecnología, Universidad Nacional de Tucumán, CP4000 San Miguel de Tucumán, Tucumán, Argentina
[b] Consejo Nacional de Investigaciones Científicas y Técnicas, CP4000 San Miguel de Tucumán, Tucumán, Argentina

ARTICLE INFO

Article history:
Received 25 February 2013
Received in revised form
15 May 2013
Accepted 28 May 2013
Available online 7 June 2013

Keywords:
Fourier analysis
Yeast
Transfer function
Overlapping index
Non-linearity

ABSTRACT

The nonlinear properties of biological suspensions have been previously presented as a bulk phenomenon without the influences of the electrodes. However, some authors have showed that the behaviour of a biological suspension is due to the nonlinear characteristics of the electrode–electrolyte interface (EEI), which is modulated by the presence of yeast cells. We have developed a method, complementary to the nonlinear dielectric spectroscopy (NLDS) which is used for the study of the behaviour of EEI with resting cell suspensions of *Saccharomyces cerevisiae*.

The method allows researchers to detect simply and quickly the voltage and frequency ranges where the metabolic activity of yeasts is detectable. This method does not replace NLDS, and aims to reduce the time during which the electrodes are exposed to corrosion by high voltages. In this paper we applied AC overpotentials (10–630 mV) with frequencies in the range from 1 to 1000 Hz. Also, we measured current harmonic distortion produced by the nonlinearity of the interface. Changes in the transfer function were observed when yeast suspension was used. Apart from the nonlinear response typical of the EEI, we also observed the biological nonlinear behaviour. The changes in the transfer functions were assessed using the overlapping index which was defined in terms of the conditional probability. The methodology was contrasted favourably with Fourier analysis. This novel strategy has the advantages of simplicity, sensitivity, reproducibility and involves basic tools such as the usual measurement of current.

1. Introduction

The nonlinear dielectric spectroscopy (NLDS) of microbiological suspensions was first proposed by Woodward and Kell (1990). They reported a biological behaviour under an applied sinusoidal electric field of less than 5 V cm^{-1} (McShea et al., 1992; Woodward and Kell, 1990, 1991a, 1991b, 1991c, 1995). They proposed a method and designed a nonlinear spectrometer for the study of the nonlinear characteristics of biological suspensions. The nonlinear spectrometer applies a sinusoidal voltage signal to a four-electrode cell through the outer electrodes and records the voltage drop between the inner electrodes. The proposed design generates two electrode–electrolyte interfaces (EEI) which have a nonlinear behaviour (Ruiz et al., 2005; Ruiz and Felice, 2007). These EEI distort the current through the cell and therefore the electric field applied is not sinusoidal. The response of the biological medium is added to the nonlinear response of the EEI. The nonlinearity of EEI was corrected with a second measuring cell, which was filled only with supernatant (without biological medium) and serves as a reference measurement. The difference between the frequency spectra of the two measurements was adopted as the nonlinear contribution of biological material. Despite the numerous attempts, the nonlinear component of EEI could not be avoided (Woodward et al., 1996, 1999, 2000). Others investigators also failed to eliminate the nonlinearity of the EEI despite using high technology systems (Nawarathna et al., 2005a, 2005b, 2006).

Treo and co-workers did measurements with an improved nonlinear dielectric spectrometer and three different electrochemical cells (Treo et al., 2005; Treo and Felice, 2009). One of them was a replica of that used by Woodward and Kell, and the other two were three- and four-electrode cells respectively. The four-electrode cell was designed to obtain an uniform electric field in the cellular suspension and low contribution of EEI due to the large area of the external electrodes. The three-electrode cell was designed to measure the impedance of EEI. They obtained variations higher than 20 dB in the third harmonic. These results indicated that the changes in the third harmonic were due to the presence of microorganisms near the EEI, and were consistent

* Correspondence to: Laboratorio de Medios e Interfases, Departamento de Bioingeniería, Facultad de Ciencias Exactas y Tecnología, Universidad Nacional de Tucumán, CC327, Correo Central, CP4000 San Miguel de Tucumán, Tucumán, Argentina. Tel./fax: +54 381 4364120.
E-mail address: gruiz@herrera.unt.edu.ar (G.A. Ruiz).

0956-5663/$ - see front matter © 2013 Elsevier B.V. All rights reserved.
http://dx.doi.org/10.1016/j.bios.2013.05.043

with Blake-Coleman's results (Blake-Coleman et al., 1994; Hutchings et al., 1994). Measurements performed with the other cells were not relevant or at least similar to Woodward and Kell's results, despite the wide range of applied electric field (0.033–30 V cm^{-1}). Interestingly, it has also been shown that the attachment of microorganisms in the EEI could produce changes in impedance measurements (Muñoz-Berbel et al., 2007, 2008a, 2008b, 2008c).

In all these studies, the harmonics in the current polarisation were analysed in frequency-domain with Fourier analysis, which is a time-consuming processing.

Moreover, the high voltages used in NLDS (above 600 mV during several minutes) led to nonlinear work zones, where the electrochemical corrosion process affects the measurement and the interpretation of results. Therefore, it is necessary to have a method which allows fast localisation of the nonlinear zones within the voltage–frequency plane to then begin a detailed harmonic analysis.

We propose a new method in the time-domain, which works complementarily with the spectrometer developed by Treo, and which aims to rapidly detect changes in the nonlinearity of the EEI. Therefore reduces the time during which the electrodes are exposed to corrosion by high voltages.

2. Materials and methods

2.1. Non-linear spectrometer

The setup consisted of a central PC to synchronize the instruments and to collect the data, an electrochemical analyser Solartron SI1287, a peristaltic pump, a magnetic stirrer (Fig. 1A) and a three-electrode measurement cell (Fig. 1B) (Treo and Felice, 2009). These sinusoidal voltage signals were applied to a biological suspension contained in the cell by means of two outer electrodes (counter electrode and working electrode).

The voltages were controlled by the electrochemical analyser to provide a sinusoidal electric field (without harmonic content) between the reference electrode and working electrode. The current flowing through the cell was sampled and transformed to the frequency domain using the periodogram method with a rectangular window (Welch, 1967). The length of the signal was chosen to ensure at least five samples of separation between harmonics. The system has been completed with a reservoir with solution and a pumping system to recirculate the solution through the cell. After complete 90 s of acquisition, the stirrer and pump were turned on for 10 s. When the inhibitor of H^+-ATPase was added to suspension, the mixture was stirred and pumped for 1 or 2 s to homogenize the system. Both the pump and stirrer were controlled by PC to ensure the steady state of system during the acquisition.

2.2. Three-electrode cell

The three-electrode cell was composed by a gold working electrode (WE), a reference electrode (RE) and a hemi-spherical stainless steel counter electrode (CE). The CE (area = 150 cm^2) was designed with an area larger than the working electrode in order to minimize its impedance. It was hermetically sealed with a thin acrylic piece (external diameter = 100 mm and diameter of the central hollow = 10 mm) containing a stainless steel wire that acts as a reference electrode (Dentaurum steel, diameter = 1 mm). This piece was supported on an acrylic disk (external diameter d = 100 mm) containing to WE (diameter = 8 mm). The WE was hand-polished before each experiment with diamond past and aluminium powder, up to a final roughness of 1 μm. The CE had tubing connections to allow the flow in and out of suspension. A magnetic stirring bar was introduced inside the cell.

2.3. Microbiological preparation

In order to compare our results with those of the other authors (i.e. Treo and Woodward), we used the same biological material (e.g. *Saccharomyces cerevisiae*). The microorganism was obtained locally as a lyophilized powder and resuspended to obtain the concentration as indicated below.

Different media were used in the assay:

1. Base solution (BS): 20 mM of KH_2PO_4, 30 mM of KCl, and 1 mM of $MgCl_2$, at pH 6.5.
2. Yeast cell Suspension (CS).
3. Stimulated cell suspension (SCS).

The CS was obtained by dissolving 3.7 g of dry yeast in 75 ml of BS and stirring for 5 min with a magnetic stirrer. SCS was obtained adding 150 μL of sodium metavanadate (SMV, 1 mM, an inhibitor of H^+-ATPase) to CS (Wach and Graber, 1991).

All chemicals used were of analytical grade and the water was glass-distilled (final conductivity less than 5 μS/cm).

2.4. Measurement protocol

AC overpotentials (10–630 mV, divided into 9 logarithmic steps) with frequencies within the interval of 1–65,000 Hz (divided into 10 logarithmic steps) were applied with the Solartron system. The experiments were carried out for the three media: BS, CS and SCS.

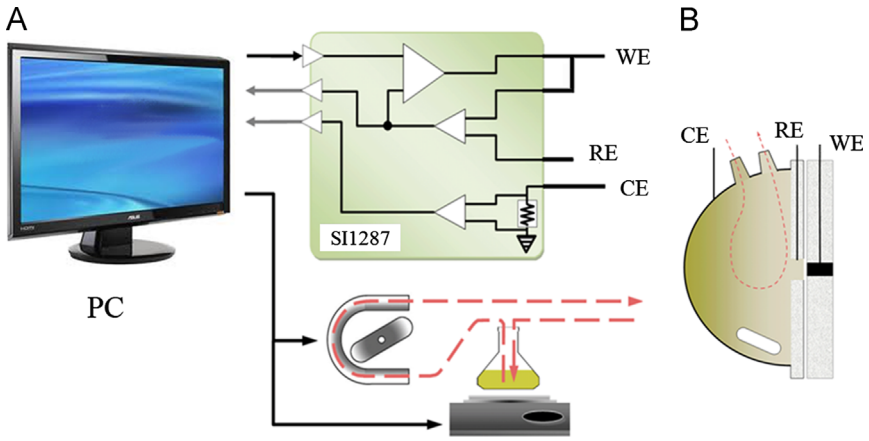

Fig. 1. Nonlinear dielectric spectrometer. (A) Equipment involved and (B) three-electrode cell. Reprinted and adapted from Treo and Felice, (2009).

The sampling frequency was such that the measurement points were equally spaced on a logarithmic scale, with 10 points per decade. The integration time of the measurements was 16 cycles. In every case, the potential was stabilised in open circuit until the open circuit potential shift was lower than 0.05 mV s^{-1}. The temperature was stabilised at 20 °C. The experiments were fully controlled by the PC. The experiments described above were repeated 5 times. In each trial, transfer function was obtained for each medium, and for each value of voltage and frequency. A transfer function is a mathematical representation of the relation between the input and output. In our case, the graphic representation of the transfer function is a closed-loop. An overlapping index $I(\cdot)$ was defined in terms of two transfer functions, which were obtained using X and Y media respectively, as:

$$I(\mathrm{X}|\mathrm{Y}) = \frac{A(\mathrm{X}\cap\mathrm{Y})}{A(\mathrm{Y})} \quad (1)$$

where X=BS, Y=CS or SCS, $A(\mathrm{X}\cap\mathrm{Y})$ represent the area bounded by the intersection of two loops corresponding to media X and Y and likewise $A(\mathrm{Y})$ represent the area inside the loop corresponding to Y medium. This definition is similar to the definition of conditional probability since, e.g. if X=BS and Y=CS, $I(\mathrm{BS}|\mathrm{CS})$ could represent the conditional probability of occurrence a change in the transfer function (obtained with BS), when yeast cells are added to the medium. $I(\cdot)$ is a dimensionless parameter and take values between 0 and 1. Values close to 0 indicate high modulations of the nonlinearity of an EEI due to metabolic activity of yeast cell. Nonlinear characterizations of the currents were also obtained. In each case all the harmonics were analysed, although in this paper only the third harmonic is presented because it proved to be the most representative of the biological behaviour (Woodward and Kell, 1991a; Nawarathna et al., 2005b). Experimental results were analysed using a factorial analysis of variance based on a fixed-effects model within the overpotential-frequency window, where the metabolic activity manifested. $I(\cdot)$ was taken as a dependent variable, while the frequency and amplitude of the applied overpotential were taken as fixed factors. It was added a third fixed factor (time) which indicates if the measurement was made before or after adding the sodium metavanadate. The p-value in relation to time was analysed, because we wanted to detect quantitative changes in the biological activity due to SMV.

3. Results

Fig. 2 shows the overlapping index $I(\mathrm{BS}|\mathrm{CS})$ for the five experiments, where X = BS and Y = CS.

The colourmap represents $I(\mathrm{BS}|\mathrm{CS})$. Then a matrix of values of $I(\mathrm{BS}|\mathrm{CS})$ was calculated using Eq. (1), which was used to construct a rectangular array of colour cells. The minimum and maximum elements of the matrix were assigned the first and last colours in the colourmap. Colours for the remaining elements in the matrix were determined by a linear mapping from value to colourmap element. Likewise the colour in each line segment and face was varied by interpolating the colourmap index across the line or face. The colourmap elected varies smoothly from black through shades of red, orange, and yellow, to white. In all experiments there was an overpotential-frequency window (white box in experiment 1 of Fig. 2) which is a region defined by the minimum values of $I(\mathrm{BS}|\mathrm{CS})$ of all experiments. Inside the window the metabolic activity of yeast cell was more manifested. Fig. 3A shows the overlapping index $I(\mathrm{BS}|\mathrm{CS})$ for the experiment 4. In this figure were selected two points at coordinates (100 mV, 56.31 Hz) and (251.19 mV, 2 Hz). The values of $I(\mathrm{BS}|\mathrm{CS})$ were very different from each other (0.975 and 0.339 respectively). Fig. 3B and C show the transfer functions for each of these points. Fig. 3D and E shows the frequency spectra of the signals of current obtained for media BS (blue) and CS (red) in the two points indicated previously. In black it is shown the difference between the two spectra above. The amplitudes of the spectra are shown in decibel. Comparing Fig. 3D with E, it can be observed that the amplitude of the third harmonic differs for these two situations. Fig. 4 shows the overlapping index $I(\mathrm{BS}|\mathrm{SCS})$ for the five experiments. In this figure it can be observed that inside the same window, (black box in experiment 1 of Fig. 4) the overlapping index values have increased significantly.

Table 1 shows a summary of the statistical analysis. This consisted of a factorial ANOVA univariate, based on a model of three fixed effects. This factorial design is typically referred to as three-way-ANOVA because three factors were taken into consideration.

The first row in Table 1 labelled “corrected model” refers to all model effects taken together (three main effects, interactions and the constant). The second, third and fourth rows include the main effects of the model. The next four rows include the effect of interactions between the factors taken in twos and threes. Time is the only main effect that is significant (p-value < 0.05).

Finally, we performed experiments to confirm that the addition of SMV does not alter the electrode behaviour. These experiments consisted of adding 150 μL of SMV in 75 ml of BS. None of them showed significant changes ($I > 0.85$).

4. Discussion

It is known that changes in the conductivity of microbiological solutions produce changes in the impedance measurements of the EEI (Treo and Felice, 2009). Thus, it was taken care that the conductivities of BS and CS were the same (5.24 ± 0.04) mS cm^{-1}. This fact was not taken into consideration by other authors (Woodward and Treo).

The changes observed in EEI due to the presence of microorganisms were repeatable and occurred in a window of low frequencies and relatively high overpotential. This window coincided with that described before by other authors (Woodward et al., 1996; Nawarathna et al., 2005b; Treo and Felice, 2009). Like them our results showed changes in the third harmonic of the order of 20–30 dB. Fig. 2 (experiment 1) shows this window as a white box.

The measurements presented in this paper are the results of the contrast between the BS and the CS or SCS. The blank measurement in this case was made with base solution (BS), i.e. without yeast. Then the measurements using yeast suspension showed changes from the blank measurement. These changes were reflected in the transfer function and were quantified by the overlap index.

The transfer function in electronics is the impedance of the system. In our case the complex impedance of the system consisted of a resistive and a capacitive part. The phase of complex impedance was different from zero for all frequencies and therefore the diagrams of overpotential versus electric current took the form of closed-loops. These diagrams are also known as the Lissajous figures. If the overpotential and electric current were sinusoidal pure, the Lissajous figures would be ellipses. Purely sinusoidal overpotentials were applied in the experiments. But even in the absence of microorganisms, the electric currents through the interface were not pure sinusoidal signals; they had harmonics (amplitude and phase) of the fundamental frequency as a consequence of the nonlinearity of the interface itself. Therefore, changes were observed in the shape, size and orientation of the closed-loops, depending on both amplitude and phase of the harmonic components (blue loops in Fig. 3B and C). When CS was used, changes in the non-linearity of the system were observed, probably due to the attachment process of microorganisms.

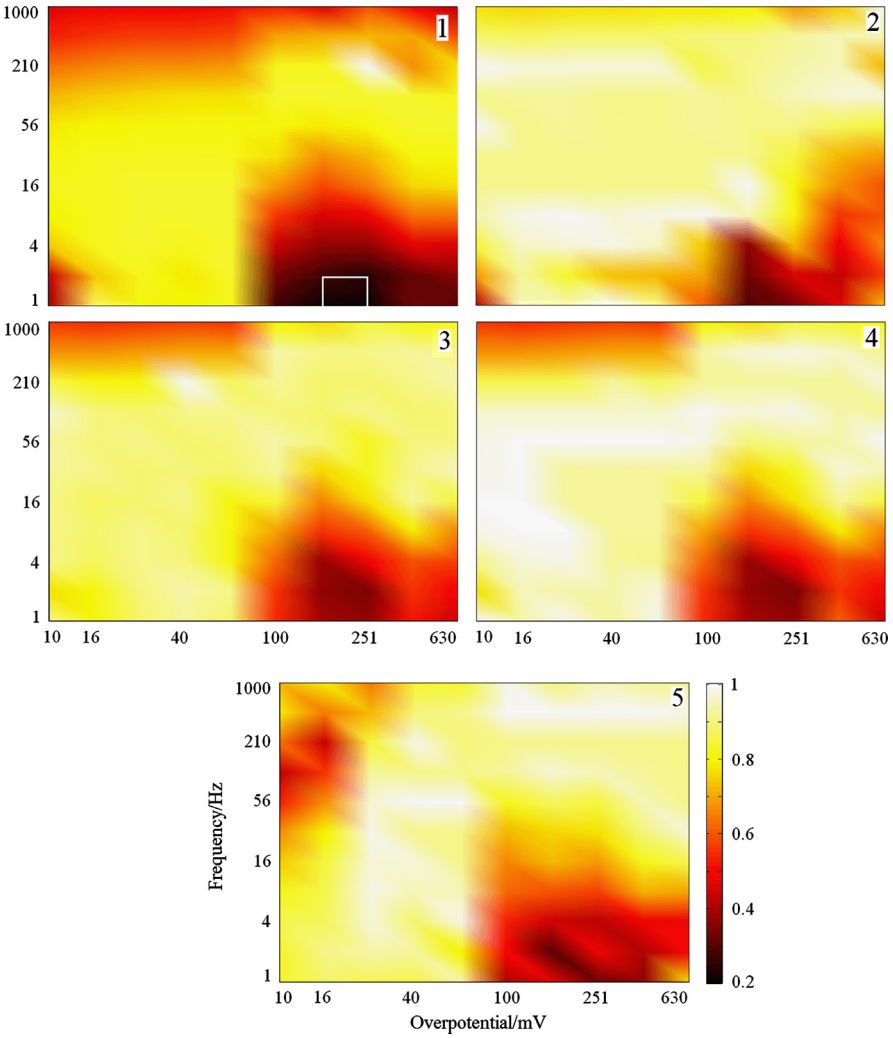

Fig. 2. Overlapping index I(BS|CS). Numbers 1–5 in the upper right vertices of each figure indicate the experiment performed. All figures have been colour-coded according to the scale shown next to experiment 5. The white box in experiment 1 is an overpotential-frequency window described for several authors. In it the values of I(BS|CS) are minimal.

As a result, other harmonics were generated which added to those typical of the interface. Hence further changes in the shape and orientation of the loops were generated (red loops in Fig. 3B and C), and thus, changes in I values (Fig. 3A). This allowed the use of the transfer function changes for overall detection of nonlinearity changes of the system. These changes were more pronounced within the overpotential-frequency window in which the metabolic activity was manifested. The spectrum obtained from the difference between BS and CS spectra, is representative of the harmonic content of the medium (black lines in Fig. 3D and E) and within the window was in the range of 20–30 dB. This harmonic was associated with the metabolic activity of the enzyme H^+-ATPase, predominantly in the cell membrane of *S. cerevisiae* (Treo and Felice, 2009). Experiments showed that inhibiting the metabolic effect of yeast cells by addition of SMV, increased the I(BS|SCS) values and tended to approximate to those values obtained with BS. This is shown in Fig. 4 (black box in experiment 1), where I(BS|SCS) values are close to 1 in the overpotential-frequency window.

In relation to the statistical analysis performed, three-way-ANOVA allowed to analyse whether changes in the frequency (first factor) or the overpotential (second factor) produced statistically significant differences in the values of $I(\cdot)$, or if the changes in $I(\cdot)$ were due to the addition of sodium metavanadate (third factor).

Moreover, the three-factor ANOVA also allowed studying the effect of the interaction between factors on $I(\cdot)$. E.g., if changes in $I(\cdot)$ due to the different frequencies remained constant, in a statistical sense, for each value of overpotential (interaction between the first and second factor), or if the observed variations in $I(\cdot)$ due to the different frequencies/overpotentials remained constant after addition of the inhibitor (interaction between first/second and the third factor).

Results in Table 1 help to validate the new method. Table 1 shows information about: the sources of variation, mean square, F-statistics and critical values (Sig.) associated with each F-statistics. P-value $= 0.000 < 0.005$ in the first row of Table 1 implies that the model explains a significant part of the observed variation in the dependent variable $I(\cdot)$.The R^2 value (0.835) indicates that all seven effects included in the model (frequency, overpotential, time, frequency × overpotential, frequency × time, overpotential × time and frequency × overpotential × time) explain 83.5% of the variance of $I(\cdot)$.

The average values of $I(\cdot)$ did not differ in the groups defined by frequency (p-value $= 0.310 > 0.05$ in the second row) and overpotential (p-value $= 0.664 > 0.05$ in the third row) factors; but they are different for the time factor (p-value $= 0.000 < 0.05$ in the fourth row). This mean that the values of $I(\cdot)$ before and after the addition of SMV are significantly different. From the fourth to the eighth row, interactions between factors taken in pairs or triples

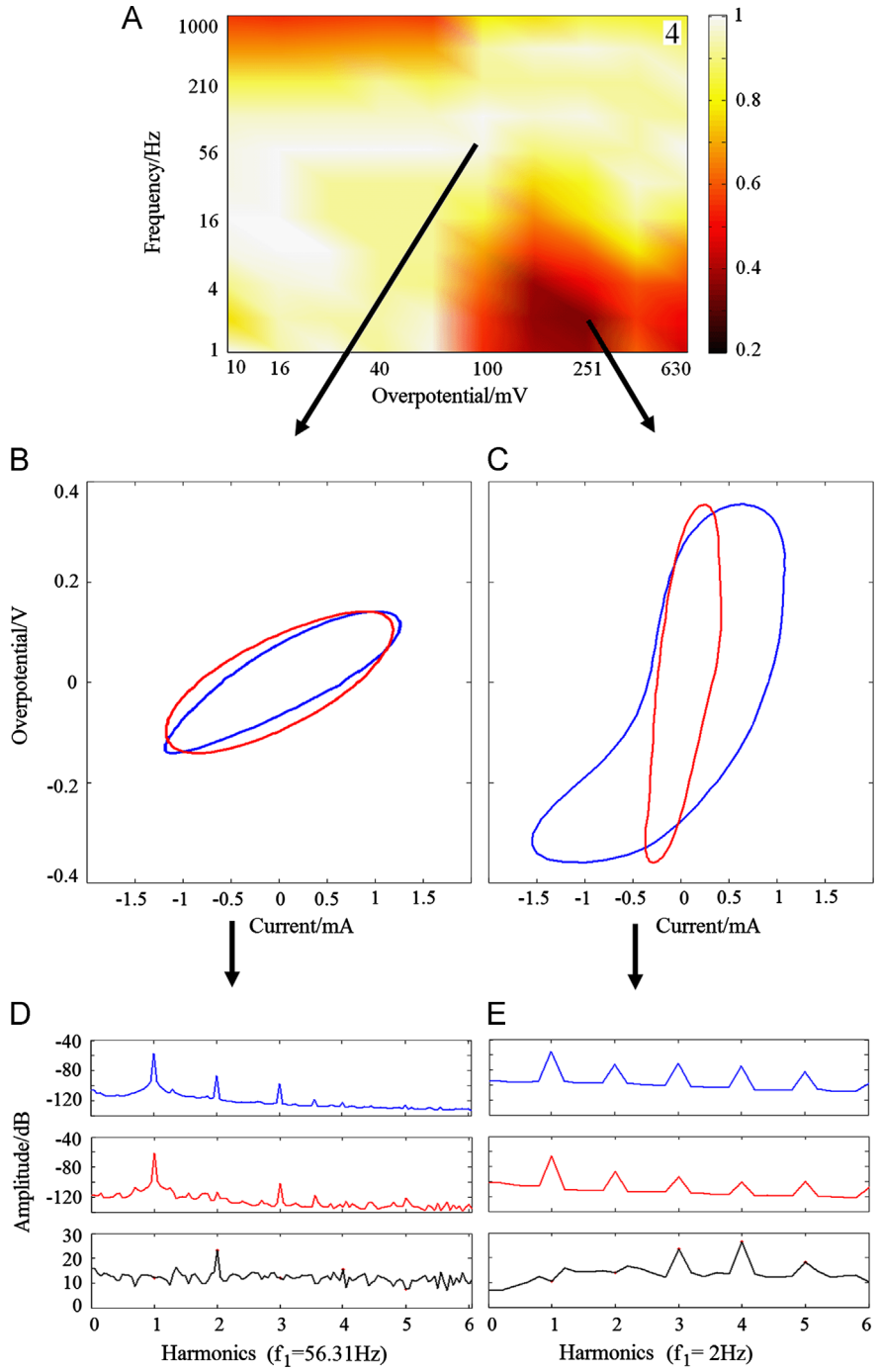

Fig. 3. Modulation of the nonlinearity of an EEI. (A) Overlapping index I(BS|CS) for experiment 4 where it was selected for two points. For the first point (100 mV, 56.31 Hz) I(BS|CS)=0.975 and for the second point (251.19 mV, 2 Hz) I(BS|CS)=0.339. (B) Shows the transfer functions obtained with the means BS (blue) and CS (red) for the first point. (C) Shows the same transfer functions as (B) to the last point. (D) Shows the frequency spectra of the current signals used in (B). In black it shows the difference between both spectra. (E) Is the same as (D) to the second point. (For interpretation of the references to colour in this figure legend, the reader is referred to the web version of this article.)

are including. The corresponding p-values (>0.05) indicate that these interactions have no significant effect on $I(\cdot)$.

Finally, it is important to remark that under our experimental conditions corrosion is a significant problem. This trouble too has been discussed by Treo and Felice (2009). They performed experiments, applying electric fields in the range from 7 V cm^{-1} to 70 V cm^{-1}. In this range and in long term experiments (above 40 min), their measurements were influenced by electrode corrosion.

The method proposed in this work allows researchers to reduce the time duration of experiments from 40 min to a few minutes, since it quickly determines nonlinear zones where metabolic activity of yeast cells is manifested. This is achieved by applying sweeps frequency and amplitude, and measuring the current flowing through the interfaces. E.g., this procedure takes as much as two minutes if the voltage is varied from 10 mV to 630 mV with frequencies between 1 and 1000 Hz, taking 10 points per decade and 5 cycles of integration.

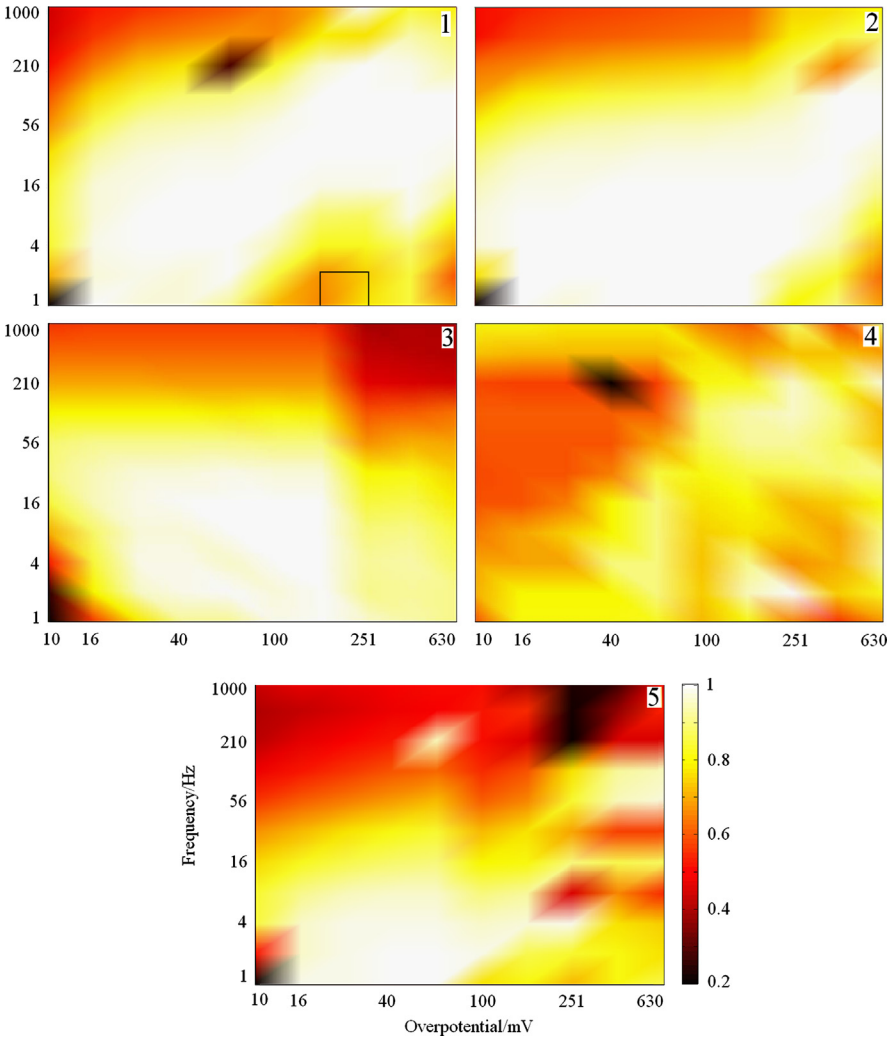

Fig. 4. Overlapping index I(BS|SCS). Numbers 1–5 in the upper right vertices of each figure indicate the experiment performed. All figures have been colour-coded according to the scale shown next to experiment 5. Here, in the black box of the experiment 1 the values of I are higher than in the white box in Fig. 2.

Table 1
Three-way-ANOVA tests of between-subjects effects (α=0.05).

Source	Mean square	F	Sig.
Corrected model[a]	.317	23.214	.000
Frequency	.015	1.064	.310
Overpotential	.003	.193	.664
Time	2.177	159.648	.000
Frequency × overpotential	.008	.610	.440
Frequency × time	.007	.507	.482
Overpotential × time	.006	.450	.507
Frequency × overpotential × time	.000	.027	.871

[a] R^2=.835; dependent variable: $I(\cdot)$.

5. Conclusions

The proposed method is simple and involves a single measurement: the electric current (or electric current density) flowing through EEI. It uses only complete cycles of overpotential and electric current. Its advantage lies in the possibility of detecting changes in the non-linearity caused by the presence of microorganisms (*S. cerevisiae*), quantifying observable changes in the transfer functions (Lissajous figures). The changes in the transfer function are quantified through the overlap index, which showed that there exists an overpotential-frequency window where the metabolic effect is detectable. When yeast cells are added, the system impedance is modulated by the metabolic activity of the enzyme H^+-ATPase. The new method shows that it is possible to monitor in a repeatable and controlled way the functioning of this enzyme membrane.

Another important issue is the fact that the proposed method significantly reduces the exposure time of the electrodes to corrosion processes by high voltages.

We must highlight that, at present, we are performing measurements designed to test the proposed method with other conditions, such as another base solution, different concentrations of the same microorganism, different kinds of electrodes (interdigitated electrodes and microelectrode both of gold) and using glucose as stimulator of the metabolic activity instead of the inhibitor. Finally, according to our preliminary results, the method is working satisfactorily.

Acknowledgements

This work was supported by grants from the Agencia Nacional de Promoción Científica y Tecnológica, the Consejo Nacional de Investigaciones Científicas y Técnicas (CONICET), and the Consejo de Investigaciones de la Universidad Nacional de Tucumán (CIUNT).

The authors would like to thank Miss Micaela García for her help in the language editing of this paper.

References

Blake-Coleman, B.C., Hutchings, M.J., Silley, P., 1994. Biosensors and Bioelectronics 9, 231–242.
Hutchings, M.J., Blake-Coleman, B.C., Silley, P., 1994. Biosensors and Bioelectronics 9, 91–103.
McShea, A., Woodward, A.M., Kell, D.B., 1992. Bioelectrochemistry and Bioenergetics 29, 205–214.
Muñoz-Berbel, X., Vigués, N., Mas, J., Toby, A., Jenkins, A., Muñoz, F., 2007. Electrochemistry Communications 9, 2654–2660.
Muñoz-Berbel, X., Vigués, N., Jenkins, A.T.A., Mas, J., Muñoz, F., 2008a. Biosensors and Bioelectronics 23, 1540–1546.
Muñoz-Berbel, X., Vigués, N., Mas, J., del Valle, M., Muñoz, F.J., Cortina-Puig, M., 2008b. Biosensors and Bioelectronics 24, 958–962.
Muñoz-Berbel, X., García-Aljaro, C., Muñoz, F.J., 2008c. Electrochimica Acta 53, 5739–5744.
Nawarathna, D., Claycomb, J.R., Miller, J., Benedik, M.J., 2005a. Applied Physics Letters 86, 23902–23903.
Nawarathna, D., Miller, J., Claycomb, J.R., Cardenas, G., Warmflash, D., 2005b. Physical Review Letters 95, 158103–158104.
Nawarathna, D., Claycomb, J.R., Cardenas, G., Gardner, J., Warmflash, D., Miller Jr., J.H., Widger, W.R., 2006. Physical Review E: Statistical, Nonlinear and Soft Matter Physics 73, 51914–51916.
Ruiz, G.A., Felice, C.J., Valentinuzzi, M.E., 2005. Chaos, Solitons and Fractals 25, 649–654.
Ruiz, G.A., Felice, C.J., 2007. Chaos, Solitons and Fractals 31, 327–335.
Treo, E., Felice, C., Madrid, R., 2005. Conference Proceedings IEEE Engineering in Medicine and Biology Society 5, 4588–4591.
Treo, E., Felice, C., 2009. Biomedical Engineering Online 8, 19–31.
Wach, A., Graber, P., 1991. FEBS Journal 201, 91–97.
Welch, P.D., 1967. IEEE Transactions on Audio and Electroacoustics 15, 70–73.
Woodward, A.M., Kell, D.B., 1990. Bioelectrochemistry and Bioenergetics 24, 83–100.
Woodward, A.M., Kell, D.B., 1991a. Journal of Electroanalytical Chemistry 320, 395–413.
Woodward, A.M., Kell, D.B., 1991b. FEMS Microbiology Letters 84, 91–95.
Woodward, A.M., Kell, D.B., 1991c. Journal of Electroanalytical Chemistry 321, 423–439.
Woodward, A.M., Kell, D.B., 1995. Biosensors and Bioelectronics 10, 639–641.
Woodward, A.M., Jones, A., Zhang, X., Rowland, J., Kell, D.B., 1996. Bioelectrochemistry and Bioenergetics 40, 99–132.
Woodward, A.M., Gilbert, R.J., Kell, D.B., 1999. Bioelectrochemistry and Bioenergetics 48, 389–396.
Woodward, A.M., Davies, E.A., Denyer, S., Olliff, C., Kell, D.B., 2000. Bioelectrochemistry 51, 13–20.